LA-UR- 08-6871

Approved for public release;
distribution is unlimited.

Title:	Shocks and finite-time singularities in Hele-Shaw Flow
Author(s):	Razvan Teodorescu/LANL/T-4/202489 P. Wiegmann/University of Montreal S-Y Lee/University of Chicago
Intended for:	Journal Physics D

Los Alamos
NATIONAL LABORATORY
EST. 1943

Form 836 (7/06)

LA-UR-07-3622

Shocks and finite-time singularities in Hele-Shaw flow

S-Y Lee,[1] R Teodorescu,[2] and P Wiegmann *[3]

[1] *Centre for Mathematical Research, University of Montreal, Montreal, Canada*
[2] *Center for Nonlinear Studies and T-4, Los Alamos National Laboratory, Los Alamos, NM 87505, USA*
[3] *The James Franck and Enrico Fermi Institutes, University of Chicago, 5640 S. Ellis Ave, Chicago IL 60637, USA*

Hele-Shaw flow at vanishing surface tension is ill-defined. In finite time, the flow develops cusp-like singularities. We show that the ill-defined problem admits a weak *dispersive* solution when singularities give rise to a graph of shock waves propagating in the viscous fluid. The graph of shocks grows and branches. Velocity and pressure jump across the shock. We formulate a few simple physical principles which single out the dispersive solution and interpret shocks as lines of decompressed fluid. We also formulate the dispersive solution in algebro-geometrical terms as an evolution of Krichever-Boutroux complex curve. We study in details the most generic (2,3) cusp singularity which gives rise to an elementary branching event. This solution is self-similar and expressed in terms of elliptic functions.

INTRODUCTION

The zero surface tension limit of Hele-Shaw flows [1] describes a planar interface between two incompressible and immiscible phases propagating with velocity equal to the density of the harmonic measure of the interface. It is a famous problem whose importance goes far beyond applications to fluid dynamics. Originally formulated by Henry Darcy in 1856 [2] in relation with groundflow of water through porous soil, it describes a large class of two-dimensional growth processes driven by a harmonic field (a.k.a Laplacian Growth) and has led to a number of important developments in mathematics and mathematical physics ranging from complex analysis to Random Matrix theory.

A compact formulation of the problem is: let $\gamma(t)$ be a simple planar curve – boundary of a single connected domain D, and $H(z)|\mathrm{d}z|$ the density of harmonic measure of the curve at a point z. The curve evolves in time t according to the

$$\text{Darcy Law}: \quad v_n(z) \sim H(z), \quad z \in \gamma(t). \tag{1}$$

Here v_n is the velocity of the curve - an outward normal vector, and $H(z)$ is the normal gradient of a solution of the exterior Dirichlet problem with a sink at a distant point of the complementary domain $\tilde{D} = \mathbb{C} \setminus D$, say, infinity:

$$H(z) = -\partial_n p(z), \tag{2}$$

$$\Delta p = 0 \quad \text{on } \tilde{D}, \quad p_{|\gamma} = 0, \quad p_{|z\to\infty} \sim -\log|z|. \tag{3}$$

Laplacian growth models [3, 4] are characterized by intricate finger-like unstable patterns [5] featuring finite-time singularities [6, 7] in the form of boundary cusp formation.

As such the problem is ill-defined: the Darcy law stops making sense, since velocity and pressure gradient diverge at a *critical point*, when a cusp-like singularity occurs.

An important feature of the Laplacian growth is its integrability. In this case, integrability means that if an initial interface is an algebraic curve of a given order, it will remain so at all times, until a critical point forms. Insights to integrability appeared in early papers [8] and then were further developed in more recent studies [9–17].

Dynamics near a critical point (i.e., close to the blow-up time) belongs to the class of non-linear problems for which any perturbation is singular. In this case various regularization schemes typically lead to different results.

This situation is typical in fluid mechanics and, in fact, similar to singularities appearing in compressible Euler flows. There, a perturbation of Euler equations by a diffusive mechanism (i.e., by viscosity) and by Hamiltonian

---

* also at the Landau Institute, Moscow

mechanism (i.e., by dispersion) lead to different physics and different flow patterns (the former transforms the Euler equation to diffusive Burgers-like equation, the latter to a Hamiltonian non-linear equation, like KdV).

A traditional laboratory set-up (called a Hele-Shaw cell after its inventor [1]) consists of two horizontal plates separated by a narrow gap, initially filled with a viscous liquid (a fluid), where inviscid liquid is pumped in at a constant rate at the center of the cell, pushing the viscous liquid away. Below we will refer to the viscous liquid as *fluid* occupying a domain $\tilde{D}$ and to the inviscid liquid as *droplet* D. Both liquids are considered to be incompressible. The droplet boundary initially moves according to the Darcy law [2], where p is the pressure of the incompressible viscous fluid. A typical pattern is seen in FIG. 1.

FIG. 1: Experimental Hele-Shaw pattern [18].

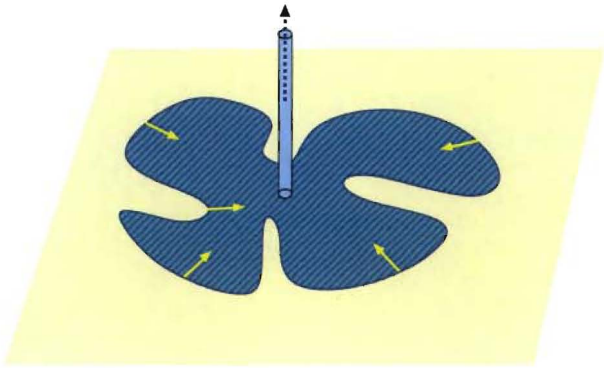

FIG. 2: Hele-Shaw flow with suction mechanism. Dashed region is oil, outside is air.

An interesting modern setting consists of a molecular thin layer of viscous liquid positioned on a horizontal wetted substrate [19] with a free boundary contracting by some suction mechanism. This liquid occupies a domain $\tilde{D}$ and we assume that a suction applied to a point of the liquid away from its boundary (FIG. 2).[46]. Advantage of this setting is that the height of the layer may vary (and indeed does vary along the boundary rim [19]), which effectively makes the two-dimensional flow compressible. Below we assume this setting but will keep the name *Hele-Shaw flow.*

It seems that the most relevant to experiments in Hele-Shaw cell [18] mechanism of taming singularities is a surface tension. Then p in (3) along the interface is proportional to its curvature. This perturbation stabilizes growing patterns (as seen in FIG. 1) but destabilizes their analytical and integrable structure. Also it is not expected that patterns possess universal features in the situation when surface tension is significant.

The traditional approach in studies Hele-Shaw flow assumes the following order of limits: the two-dimensional density of the fluid is set to a constant first, then singular patterns are regularized by surface tension. In this case, the limit of surface tension going to zero is ill-defined; the solution blows up.

Another kind of perturbation to Laplacian growth is suggested by the model of Diffusion-Limited Aggregation (DLA) [20] or iterative conformal maps algorithm [21]. There the interface evolves by coalescence (aggregation) of Brownian walkers supplied at a constant rate from a marked point (infinity). The probability of aggregation at a given point is proportional to the harmonic measure of the existent aggregate. In the limit when the area of a particle tends to zero, the problem of aggregation becomes identical to the Laplacian growth. Aggregation continues beyond this limit, producing notoriously intriguing fractal patterns, FIG. 3. In this case, the zero-size limit for particles leads to a singular perturbation problem.

FIG. 3: Typical Diffusion Limited Aggregation pattern.

This model has two distinguished features:

- the growth has a geometrical nature. It is determined only by the harmonic measure of the interface and, contrary to the regularization by the surface tension, does not depend on the curvature of the interface;

- due to a finite size and irregular shape of particles the limit of aggregation model to the continuos fluid mechanics effectively leads to a compressible fluid.

The geometrical regularization suggested by the aggregation models is a primary motivation of this paper (and also preceding papers [9–17]). We will assume that fluids are compressible and then study a singular limit when compressibility vanishes, setting surface tension to zero in the first place. We will argue that:

- there is a dispersive (or Hamiltonian) regularization of singularities when the problem remains integrable and well posed. Integrability allows to keep a full control on the singular solutions; under dispersive regularization fluids are assume to be compressible;

- formation of a cusp-like singularity is followed by *shocks* – lines of finite discontinuity of the density, pressure and velocity, propagating through the fluid;

- shock lines form an evolving branching pattern. Patterns of shocks, although transcendental, is controlled by the algebraic geometry of the initial, smooth curve.

In a subsequent publication we will describe the connections between weak solutions of the Hele-Shaw problem and a few related mathematical problems. We will show that:

- the lines of discontinuities (shock fronts) correspond to accumulation of zeros of bi-orthogonal polynomials;
- the shock fronts are anti-Stokes lines of isomonodromy problem naturally related to the Whitham averaging of solutions of Painlevé equations corresponding to the integrable models associated with particular types of cusps.

Shock fronts typically form a branching tree. In this paper we provide a detailed analyses of the shock pattern solution representing the birth of the first branching event of what will become a complicated degree-two tree. This solution is self-similar and represents a local structure of branching of a developed tree. A growing tree of shocks resembles DLA branching patterns. We intend to make a detailed comparison with DLA in the future, although a global structure of the branching graph (beyond its simple topological structure) is a challenging mathematical problem.

Shock solution of the flow is understood as *weak solutions* of the Hele-Shaw problem. It is a realization of dispersive regularization of the problem suggested in earlier papers of the authors [47].

A comment is in order: typically, shock waves in hydrodynamics are associated with phenomena occurring at high Reynolds numbers, due the inertial term in Euler equations [22, 23]. Here we encounter a new situation when a discontinuous solution occurs in a viscous flow where the Reynolds number is small and inertia terms are neglected in the Navier-Stockes equations [18]. From this point of view perhaps a "crack" rather than a "shock" is a better name for a discontinuity of this kind.

It is unlikely that shocks can be seen in a traditional Hele-Shaw cell with a traditional composition of two fluids. In current experiments [18] the surface tension seem to run the pattern. A more promising setting occurs when a thin layer of a fluid or a miscible composition of fluids expanding on a flat neutral substrate [19]. Another interesting setting occurs when air propagates through granular media [24].

The paper consists of three parts: first we review known facts about singularities in the Hele-Shaw flow and formulate the flow in terms of *inverse balayage* - in important concept giving insights to the weak solution. Then we formulate the problem of *weak dispersive solution* which allows shocks, describe hydrodynamics of shocks and formulate the flow in terms of evolution of complex curve. Finally we give a detailed analysis of a generic (2,3) - cusp singularity and describe an elementary branching event. This solution fully illustrate the nature of dispersive solution.

PRELIMINARIES

Hele-Shaw flow

A thin layer of viscous fluid of the hight b occupies an open domain $\tilde{D}$ with a smooth simply-connected boundary $gamma(t)$. The fluid is sucked from a point $z = \infty$ at a constant rate Q.

We assume that the flow is quasi-stationary and neglect the $\frac{\partial \mathbf{v}}{\partial t}$ term in the in the Navier-Stockes equation in both liquids $\rho\left(\frac{\partial \mathbf{v}}{\partial t} + \mathbf{v}\cdot\nabla\mathbf{v}\right) = -\nabla p + \mu\nabla^2\mathbf{v}$, where $\mu = \nu\rho$ is the dynamic viscosity, ν the kinematic viscosity, and ρ the density of the liquid. In the viscous fluid we also assume that the Reynolds number is small $Re = |\mathbf{v}|b/\mu \to 0$, and further neglect the inertial term there. We obtain $\mu\nabla^2\mathbf{v} = \nabla p$. Of course this approximation is consistent if the fluid is irrotational $\nabla \times \mathbf{v} = 0$ as it is seen from the last formula. Assuming a Poisseulle profile for a flow we replace and $\nabla_z^2\mathbf{v}$ by its average $-(12/b^2)\mathbf{v}$ and neglect $(\nabla_x^2 + \nabla_y^2)\mathbf{v}$ we obtain Darcy law

$$\rho\mathbf{v} = -K\nabla p, \tag{4}$$

where $K = \frac{b^2}{12\nu}$ is called *hydraulic conductivity*. Incompressibility of the viscous fluid $\nabla\cdot\mathbf{v} = 0$ and (4) imply that pressure in fluid is a harmonic function at constant density

$$\Delta p = 0 \quad \text{in } \tilde{D}, \tag{5}$$

where we assume that K and ρ are constants. We will relax the condition of constant density when defining weak solutions. The fluid is sucked with a constant rate $Q = -\oint_\gamma \rho\mathbf{v}\times \mathrm{dl}$, where γ is oriented counter-clockwise. According to the Darcy law (4), it equals $K\oint_\gamma \nabla p \times \mathrm{dl}$.. Therefore at the drain $p \to -\frac{Q}{2\pi K}\log|z|$ as $z\to\infty$.

If the boundary is smooth, the pressure on the boundary is controlled by the surface tension $p = \sigma \times$ curvature. If the surface tension vanishes, the pressure is constant along the boundary and is Dirichlet harmonic function in the fluid.

It is instructive to compute the normalized power required suck the fluid $N(t) = -\int_{\tilde{D}} \rho \nabla p \cdot \mathbf{v} \mathrm{d}x\mathrm{d}y$. Darcy law yields that the power is the Dirichlet integral

$$N(t) = K \int_{\tilde{D}} (\nabla p)^2 \mathrm{d}x\mathrm{d}y. \tag{6}$$

The contribution to the integral comes from the boundary of the domain and from the drain

$$N(t) - N_0 = -\frac{Q^2}{2\pi K} \log r(t) - \oint_\gamma \rho p \mathbf{v} \cdot \mathbf{dl}, \tag{7}$$

where we subtract a time independent contribution $N_0 = (Q^2/2\pi K) \log R$ depending on the size of the cell R. Here $r(t)$ is a *conformal radius* of the droplet defined as $\log[r(t)/R] = -(2\pi K/Q)p|_R, R \to \infty$ (see the next section for another the definition).

If pressure vanishes at the boundary, which is before the critical point, the contribution of the boundary integral also vanishes. The total power $N - N_0 = -(Q^2/2\pi K) \log r(t)$ measures the conformal radius of the droplet.

We will see that the pressure no longer vanishes along shocks and contributes to the power. We will see that, as the systems approaches a cusp singularity and then enters into a shock regime, the power required to produce the flow will increase with a discontinuous slope, every time when shock front branches.

Finite-time singularities in Hele-Shaw flow

The dynamics described by the Darcy law (1, 2) is ill-defined. This has been understood from different angles [5, 8, 25], and can be seen from a simple argument: let $w(z)$ is a conformal univalent map of the fluid domain $\tilde{D}$ onto the exterior of the unit circle, $|w| > 1$; then the exterior Dirichlet problem has an immediate solution

$$p(z) = -\frac{Q}{2\pi K} \log |w(z)|, \quad \rho v = \frac{Q}{2\pi} |w'(z)|, \ z \in \tilde{D}. \tag{8}$$

In other words, velocity of a point of a boundary is proportional of the density of harmonic measure $H(z)|\mathrm{d}z| = |w'(z)||\mathrm{d}z|$ of that point. As a consequence, a sharper (more curved) part of the boundary moves with a higher velocity than the rest, such that the sharper part is getting even sharper before it becomes singular. This occurs for a generic initial data, although a number of exceptions are known [26]. We will demonstrate this mechanism on a simple but representative example below, but first we remind the major feature of the dynamics [8, 25]: let us denote by

$$t_k = -\frac{\rho}{k\pi} \int_{\tilde{D}} z^{-k} \mathrm{d}x\mathrm{d}y = \frac{\rho}{2\pi \mathrm{i} k} \oint_\gamma z^{-k} \bar{z} \mathrm{d}z \tag{9}$$

the harmonic moments of the fluid, and the area of the area of the plane not occupied of the fluid (domain D) is $\pi t_0/\rho = Q \cdot t$. Parameters $\{t_k\}$ are called *deformation parameters*. It follows from the Darcy law that [8]

$$\dot{t}_k = 0.$$

From now on we set $K = 1, Q = \pi$, but keep ρ as a parameter to help to control dimensions of formulas. In these units the area is just equal to $\pi \times$ time.

Let us write the inverse (time-dependent) map as

$$z(w) = rw + \sum_{k \geq 1} u_k w^{-k}, \quad |w| \geq 1, \tag{10}$$

where the coefficient r, chosen to be real positive is the conformal radius. According to a standard formula of complex analysis the coefficients of the inverse map determine the area of the domain D, which we denote by πt, through

$$t = r^2 - \sum_{k>0} k|u_k|^2. \tag{11}$$

Let us consider a simple example of a domain D whose shape is given by a hypertrocoid - an algebraic curve with a three-fold symmetry such that all harmonic moments vanish $t_k = 0$, except for the third one t_3:

$$z(w) = rw + \frac{u}{w^2}. \tag{12}$$

The ratio between the square of conformal radius r and u can be expressed through t_3, as $u = 3(\bar{t}_3/\rho)r^2$. Then the area formula reads $t = r^2 - 18(|t_3|/\rho)^2 r^4$.

Clearly, this polynomial in r^2 reaches the maximum $t_c = r_c^2/2$ at $r_c = \rho/(6|t_3|)$, and can not increase further. At this moment the hypertrocoid develops three simultaneous cusp-like singularities FIG. 4.

The mechanism of the evolution toward a critical point is: a critical point of the inverse map $z'(w_c) = 0$ is located inside the droplet $w_c = (2u/r)^{1/2} = (r(t)/r_c)^{1/2} < 1$ and moves in time towards the boundary. At a critical time the critical point reaches the boundary, say at $w = 1$. In the critical regime, when the critical point of the conformal map is already close to the boundary $z(w)/r_c|_{w=e^{i\phi}} - \frac{3}{2} = x(\phi) + iy(\phi)$, the boundary locally is approximated by a *real degenerate elliptic curve*

$$X(\phi) := \frac{2}{3}x(\phi) \approx e(t) - \phi^2, \qquad Y(\phi) := 4y \approx 2\phi^3 - \frac{3}{2}e(t)\phi, \tag{13}$$

$$Y^2 = -4\,(X - e(t))\left(X + \frac{e(t)}{2}\right)^2, \qquad e(t) = -\frac{4}{3}(1 - \frac{r}{r_c}) = -\frac{2}{3}\left(1 - \frac{t}{t_c}\right)^{1/2}. \tag{14}$$

At a critical point $t = t_c$ the curves degenerates further to a (2,3) cusp

$$Y^2 \sim X^3. \tag{15}$$

Close to the critical point conformal radius depends on time in a singular manner as $r/r_c - 1 \approx -\frac{1}{2}\,(1 - t/t_c)^{1/2}$, so that the time dependence of power becomes non-analytic: $N - N_c \approx -\frac{1}{2}\,(1 - t/t_c)^{1/2}$.

Once the (2,3) singularity occurs, the shape of the pre-cusp finger is given by the elliptic curve (14). Up to a scaling of coordinates and time the curve is universal - it does not depend on details of the original domain:

$$Y(X,t) = \left(1 - \frac{t}{t_c}\right)^{3/4} Y\left(\frac{X}{(1 - \frac{t}{t_c})^{1/2}}\right) \tag{16}$$

Self-similarity is preerved after the flow passes through the critical point $t > t_c$.

This simple analysis has a straightforward generalization for all cases where a *finite* subset of $\{t_k\}_{k>0}$ is non-vanishing. At least for this class of initial conditions described below, a flow leads to cusp-like finite-time singularities. For purposes of analysis of singularities it is sufficient to consider only this set of domains. Of course, the class of initial conditions which leads to singularities is much wider. We do not attempt to classify it here. We only mention that domains with a finite number of non-zero exterior harmonic moments belong to the class of *generalized quadrature* domains. For generic properties of generalized quadrature domains, see e.g., [27].

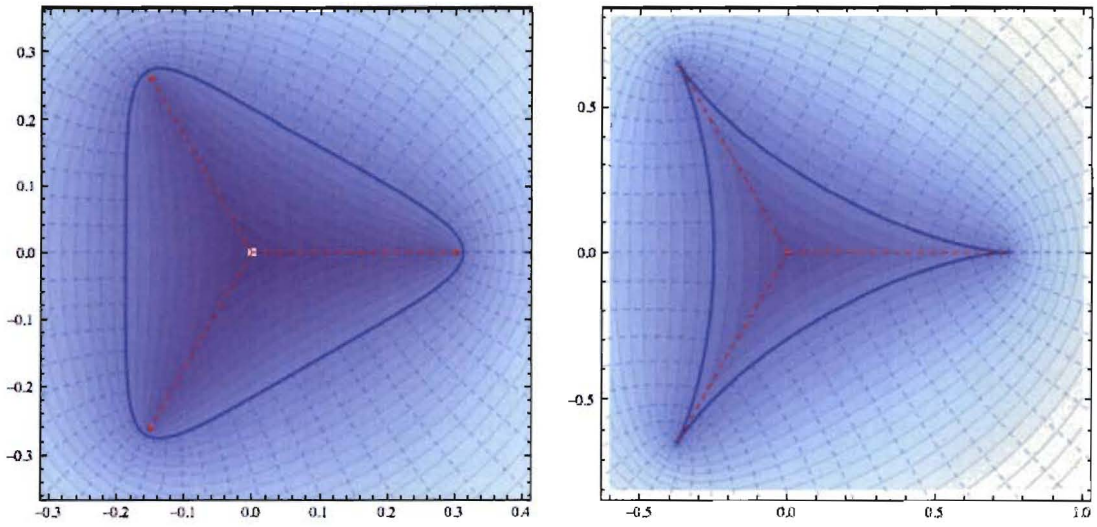

FIG. 4: Symmetric hypertrochoid (12) evolving under Darcy law (left) reaches the (2,3)-cusp singularities (right) when all three critical points (red dots) hit the boundary at the same time. The shaded contour lines are the equi-pressure lines. The dashed lines are the stream lines. The red dashed lines are branch cuts - *a skeleton.*

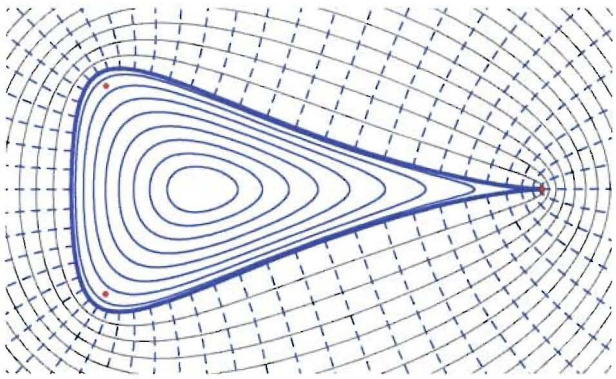

FIG. 5: Deformed hypertrochoid $z(w) = r\,w + \frac{A_r}{2r} + \frac{A_r}{w} + \frac{r^2}{w^2}$ with $A_r = r - 4r^3 - \sqrt{\frac{3r^2}{5} - 8r^4 + 16r^6}$, where one critical point gives rise to (2,3) singularity while two other critical points remain in the domain D. Closed lines inside the critical boundary show the pre-critical evolution.

The first classification of singularities

The fact that for rather general initial data, the boundary evolves to a cusp-like singularity has been noticed already in the earlier papers [25, 28] where the model of Laplacian growth has been originally formulated. Further developments are due to Refrs. [5, 29] and [3, 7, 30, 31] and [32]. For the most generic initial condition a cusp (2,3) occurs. Higher-order cusps and corner-like singularities require special initial conditions.

In Ref. [32] it was shown that only cusps $(2, 2l+1)$: $y^2 \sim x^{2l+1}$, can occur in simply connected generalized quadrature domains. Moreover, in [33] it was shown that in the critical regime a finger developing these cusps is described by a *real degenerate hyperelliptic curve*

$$Y^2 = -4(X - e_i(t)) \prod_{i=1}^{l} (X - d_i)^2, \tag{17}$$

where the double roots d_i (*double points*) all located in the fluid domain and a single critical point is located outside of the fluid (another critical point – required by the Riemann-Hurwitz theorem – is found far away from the critical region, and it plays no role in the analysis). The condition that no critical points are found in the fluid, necessarily means that the exterior critical points coincide, giving double points, such that the complex curve is degenerate. A cusp of type $(2, 2l+1)$ occurs when a branch point - a real root of e_i merges with l double points found outside the droplet.

For a reference we give here explicit formulas for the generic hyperelliptic curve (17) following the Hele-Shaw evolution [33]. The curve depends on l deformation parameters $\{t_{2k+1}\}, k = 1, \ldots, l$ (not to be confused with the harmonic moments t_k) and it is uniformized by the formulas

$$X = \phi^2 - e(t), \quad Y = \sum_{n=1}^{l+1} (n + \tfrac{1}{2}) t_{2n+1} \sum_{k=0}^{n-1} \frac{(2n-1)!!}{(2n-2k-1)!!} \frac{(-e(t))^k}{2^k k!} \phi^{2n-2k-1}, \tag{18}$$

$$t_1 + \sum_{k=1}^{l+1} \frac{(2k+1)!!}{2^k k!} t_{2k+1} (-e(t))^k = 0. \tag{19}$$

Here t_1 is the time before the cusp singularity, $t_1 \sim t_c - t$, and we set $t_{2l+3} = 4/(2l+3)$.

For a discussion of more complicated algebraic cusp singularities of the type (p, q), $X^p \sim Y^q$, see Ref.[32].

In Ref. [30] it has been argued that dynamics can be continued through a cusp of the type $(2, 4k+1)$ for the price of an appearance of an unstable point when a boundary touches itself. Another stable solution was found in [17]) when the fluid undergoes a *genus transition*: it becomes multiply connected.

However in the case of the most generic cusp (2,3) and its descendants $(2, 4k-1), k > 0$, no smooth solutions are possible. This situation is the subject of this paper.

Algebro-geometry formulation

Schwarz function

We briefly review some elements of the algebro-geometric description of the Hele-Shaw flow. It is based on the notion of the Schwarz function and differentials related to the Schwarz function. As we have said, to study local behavior of an isolated cusp, it is sufficient to consider domains with a finite set of non-zero harmonic moments (9).

The Schwarz function of a simple planar closed curve (a boundary of the fluid) γ is an analytic function in a strip surrounded the γ such that on the boundary

$$S(z) = \rho\bar{z}, \quad z \in \gamma. \tag{20}$$

It is represented by the Laurent series with respect to a drain at infinity and an arbitrary point, say $z = 0$ inside the droplet

$$S(z) = S_+(z) + S_-(z), \tag{21}$$

The positive part is an analytic continuation through the boundaryof the electric field produced by a uniformly charged fluid domain outside of the fluid $S_+|_{z\in D} = \frac{\rho}{\pi}\int_{\tilde{D}} \frac{\mathrm{d}x\mathrm{d}y}{z-\zeta}$, $\zeta = x + \mathrm{i}y$. It encodes information about the moments of exterior ([34]). We assume it to be a polynomial

$$S_+(z) = \sum_{k>0} k t_k z^{k-1} \tag{22}$$

The negative part $S_-(z)$ is an analytic continuation of the electric field produced by a uniformly charged domain D to the fluid domain as $S_-|_{z\in\tilde{D}} = \frac{\rho}{\pi}\int_D \frac{\mathrm{d}x\mathrm{d}y}{z-\zeta}$. As we have said, the coefficients t_k, and, therefore, the positive part of the Schwarz function do not evolve. They can be read from initial data of the flow.

It follows that the time derivative of the Schwarz function is holomorphic in the fluid. On the boundary, it is equal to twice the velocity on the boundary (this follows from (20)). Together, it means that the velocity of the fluid and the time derivative of the Schwarz function are related by: $2v = \partial_t S(z)$, where $v = v_x - iv_y$. In complex notation (from here on we set $t_0 = t$) the Darcy law reads:

$$2v(z,t) = \partial_t S(z,t), \tag{23}$$

$$\partial_t S(z,t) = 2\mathrm{i}\partial_z \phi(z,t), \tag{24}$$

where

$$\phi(z,t) = \psi(z,t) + \mathrm{i}p(z,t) \tag{25}$$

is the potential of the flow, whose imaginary part is the usual scalar pressure p, and the real part is the stream function ψ. In the fluid they are harmonic conjugated functions, the potential is analytic function.

Another way to formulate Darcy law is to say that the form $\mathrm{d}\omega = S\mathrm{d}z + 2\mathrm{i}\phi\mathrm{d}t$ is closed.

Close to a cusp, it is convenient to describe the boundary in Cartesian coordinates $Y = \frac{1}{2\mathrm{i}}(z - S(z))$ and $X = \frac{1}{2}(z + S(z))$, and treat Y as a function of X. In these coordinates (and up to an exact form), $\mathrm{d}\omega = -2\mathrm{i}(Y\mathrm{d}X - \phi\mathrm{d}t)$ and the Darcy law (23) reads:

$$\partial_t Y(z,t) = -\partial_X \phi(X,t). \tag{26}$$

Furthermore, it is convenient to choose the cusp as an origin and to redefine the time $t \to t_1 \sim t - t_c$ and deformation parameters relative to the cusp. Then, in the case of the cusp $(2, 2l+1)$ the hyperelliptic curve (17) is represented by the Laurent series with respect to the local parameter at infinity $X^{1/2}$

$$Y(X) = Y_+(X) + Y_-(X), \tag{27}$$

$$Y_+(X) = \textstyle\sum_{k=0}^{l+1}(2k+1)t_{2k+1}X^{k-1/2}, \tag{28}$$

where Y_- consists of negative powers in $X^{1/2}$. Darcy law then states that the positive part is conserved:

$$\dot{Y}_+(X) = 0. \tag{29}$$

Eqs. (17) are solution of the Darcy law written in the form (26) under assumption (27). The parameter ϕ in (17) (treated as a function of X) is a complex potential of the flow at the point $z = X + iY$.

If the number of non-zero harmonic moments is finite, the Schwarz function (21) has only a finite-order multiple pole at infinity and the only singularities inside the droplet are moving branch points. Moving branch points of the Schwarz function are critical points of the inverse conformal map $z(w)$ that we follow. They encode the entire flow. This situation, although not being the most general, occurs in the critical regime, next to a cusp-singularity.

In this case, there is a unique special way to draw branch cuts. They can be drawn as a (possibly multi-component) curved graph $\Sigma_k(t)$ such that the jump of the differential $-\mathrm{id}\Omega = -\mathrm{i}S\mathrm{d}z$, being canonically (counterclockwise) oriented along the curve through every branch cut, will be real and positive

$$-\operatorname{idisc} S(z,t)\mathrm{d}z = 2\sigma_k^{(1)}(z,t)|\mathrm{d}z| > 0, \quad z \in \Sigma_k(t). \tag{30}$$

Here the differential is taken along the cut and $|\mathrm{d}z|$ is an element of an arclength along a cut. The canonical orientation (important for all signs in formulas below) is depicted in FIG.6.

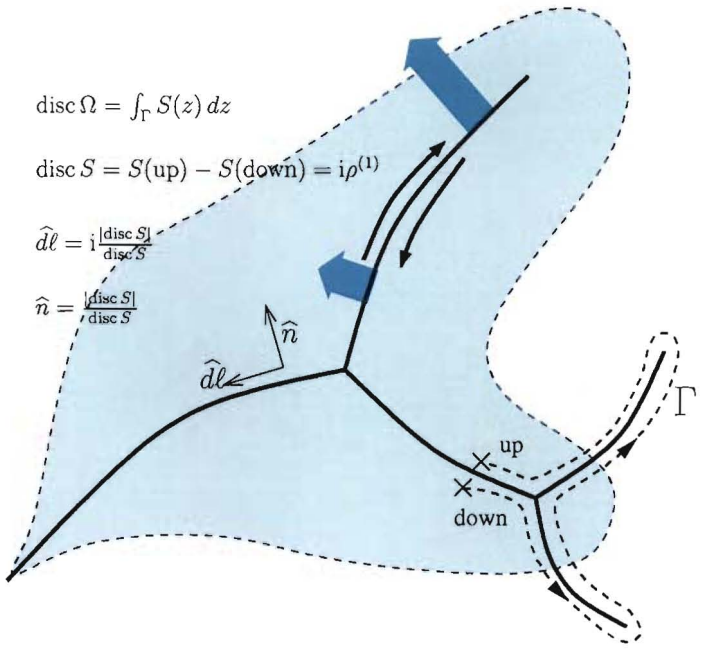

FIG. 6: Schematic graph of shocks (thick lines), fluid (air) domain (shaded region). In the figure, we show the three possible stages of evolution: i) when the branch point is inside the air domain, ii) when the air domain forms a cusp, and iii) when the shock develops after the cusp. We show the canonical orientation of the contour (dashed line Γ) to define the discontinuity of, say, S and Ω. See the formula inside the figure. We also show the unit vectors $\widehat{d\ell}$ and $\widehat{n}$ which are respectively parallel and perpendicular to the shock. Lastly, we show the normal velocity of the shock by the thick arrows and the flow of "anti-oil" (that goes in opposite direction of oil) around the shock by thin arrows. The arrows schematically show that "the sum of vorticity from the shock and from the surrounding" is zero. Though not in the figure, we also mention that the normal velocity is to the side of lower pressure.

This fact is equivalent with the following analytical continuation of the negative part of the Schwarz function to the domain D:

$$S_-(z) = \sum_k \int_{\Sigma_k} \frac{\sigma_k^{(1)}(\zeta)}{z-\zeta}|\mathrm{d}z|, \tag{31}$$

with $|\mathrm{d}z|$ the arclength measure. In other words the negative part of the Schwarz function is the electric field produced by a single layer of charges $\sigma_k^{(1)}$ distributed along a graph Σ. An important theorem on generalized quadrature domains [35] tells that this is possible and unique. The curved and generally multiply connected graph $\{\Sigma_k\}$, confined in the domain D, is called *skeleton* or *mother-body* [35]. Line densities of the skeleton depend on time only through time dependence of the branch points. If a branch point $e(t)$ is simple (which we assume), the line density $\sigma_k^{(1)}(z,t)$ vanishes

at the branch point by a *semicircle law* as

$$\sigma^{(1)}(z,t) \sim \sqrt{|z-e(t)|} \tag{32}$$

In the case of the hypertrocoid, the graph consists of three curved lines connected the branch points. They are drawn on the Fig. 5. In the case of symmetric hypertrocoid the special branch are three straight lines (FIG.4)connecting the branch points $e(t) = \frac{3}{2} r_c \left(r(t)/r_c\right)^{4/3} \times (1, e^{\pm i 2\pi/3})$ with the line densities at the branch points $4(2/3)^{1/2} r_c (1 - r^2/r_c^2)(r_c/r)^{2/3}[\sqrt{|z-e(t)|} + (4/3)(r_c/r)^{4/3}|z|/r_c\sqrt{|z-e(t)|}]$ (where z is measured from the corresponding local position of a cusp).

The major property of a generalized quadrature domains (actually serving as its definition) [27] is: area averaging of an integrable analytic function $f(z)$ over any domain B is reduced to counting of singularities of the Schwarz function $\frac{1}{\pi}\int_B f(z)\rho dxdy = \frac{1}{2\pi i}\oint_{\partial B} f(z)S(z)dz = \frac{1}{2\pi i}\oint_{\partial B} f d\Omega$. This follows from the representation (31) above:

$$\frac{1}{\pi}\int_B f(z)\rho \mathrm{d}x\mathrm{d}y = \frac{1}{2\pi i}\oint_{\partial B} f(z)S(z)dz = \sum_k \int_{\{\Sigma_k\}\cap B} \sigma^{(1)}(\zeta) f(\zeta)|\mathrm{d}\xi|. \tag{33}$$

If the domain B does not contain moving singularities or the drain, then the average stays constant in Hele-Shaw flow. Conversely, if the domain B contains moving singularities, or a drain, the average depends on time. The inverse of the procedure we just described is known as *balayage* [35]. A Newton potential created by uniformly distributed mass through the droplet measured outside of the droplet, in $\tilde{D}$, will be the same as the Newton potential created by the (non-uniform) line densities $\sigma^{(1)}$.

The balayage procedure allows the following insightful interpretation of Hele-Shaw flow. The "skeleton" – moving branch cuts – may be considered as time-dependent sources of the viscous fluid. In this interpretation there is no smooth droplet of air, only time-dependent line sources. An extended fluid occupies all the plane except the sources and moves with velocity $v = (1/2\rho)\partial_t S$. The pressure of the extended fluid than is defined by $\rho v = -\nabla p$. The original boundary then can be restored (if necessary) as a *real oval* of the complex curve - a planar curve where $S(z) = \rho\bar{z}$, or (equivalently) a zero-level set of the pressure $p = 0$. Darcy Law (23,24) then applies both inside and outside the droplet.

In this interpretation the entire flow is encoded by the motion of the skeleton, or rather by the motion of end points of the skeleton. Moreover, velocity and pressure and stream function generally have finite discontinuities across the skeleton. Also, the pressure may not be constant along the sides of the skeleton, while velocity is not normal to the skeleton.

A singularity occurs when a growing skeleton hits the boundary of the fluid.

In the next section where we formulate a weak solution of the Hele-Shaw flow we will derive equations for moving shock graph. Same equations are applied for a moving skeleton.

WEAK SOLUTIONS OF HELE-SHAW PROBLEM

As we have discussed, once the flow reaches a (2,3)-cusp singularity, it can not be continued any longer. The Darcy law written in a differential form looses it sense at the cusp - harmonic measure there diverges.

This situation is typical for differential equations ([36–39]) of the form of conservation laws of *hyperbolic type*:

$$\partial_t u + \nabla f(u) = 0 \tag{34}$$

These equations are ill-posed. There Cauchy problem with smooth initial data, leads to singularities developing in finite time (such as shocks, vortices, etc.). Darcy equation written in the form (24) is of this type, with $u = S$, $f = -2\mathrm{i}\phi$.

The origin of this phenomenon is that conservation equations of the hyperbolic type are an approximation of a well-defined problem. Deforming these equations by adding terms with higher gradients, controlled by a small parameter $\hbar$, will prevent formation of singularities. If a smooth solution of a deformed equation $u|_\hbar$ leads to a space-time discontinuous function $u|_{\hbar\to 0}$ as a deformation removed, it is called a weak solution. A discontinuity (a shock) travels with the velocity given by the Rankine-Hugoniot condition [23]

$$V = \frac{\mathrm{disc}\, f}{\mathrm{disc}\, u}, \tag{35}$$

a weak form of the differential equation (34).

In most cases, simple physical principles allow one to construct a weak solution without actually specifying the regularizing deformation. The best known example is the Maxwell rule determining the position of shock front [22], or more generally, the Lax-Oleynik entropy condition for the so called *viscous solution* of equations with hyperbolic conservation laws [36–39].

Here we assume the same strategy. We will be looking for weak solutions of the Hele-Shaw problem when the Darcy law is applied everywhere in the fluid except a moving, growing and branching graph $\Gamma(t) \subset \tilde{D}$ of shocks or cracks where hydrodynamic variables pressure and velocity suffer a discontinuity - a weak form of singularity.

We will show that very simple and natural physical principles guide us to an unique weak solution. which we will call *a dispersive solution.* The inverse balayage discussed in the previous section gives necessary insights.

From a physical point of view, the shocks are narow extended channels with a deficit of fluid. They communicate with the bulk of the fluid supplying/removing fluid to/from the bulk. In the case of $(2, 4k-1)$ cusp singularities, which we consider here, shocks are connected to the boundary. Obviously this may happen if the condition that the density of the fluid is a constant must be relaxed. A difference between shocks and a regular boundary is that pressure and velocity of the fluid both have steep gradients (controlled by the parameter $\hbar$) through a shock. Also the pressure does not stay constant along the shock line.

Weak form of Darcy law: the Rankine-Hugoniot condition and admissibility

Since velocity of the fluid jumps through the shock, so does the Schwarz function (defined by $2\rho v = \partial_t S$).

Thus the Schwarz function, being analytic everywhere in the fluid (under assumption that the S_+ is a polynomial as is in (22)), has branch cuts inside the domain D, now, after a critical time has been passed, also has branch cuts in the fluid domain $\tilde{D}$. We write

$$S_-(z) = \frac{1}{\pi}\int_D \frac{\rho \mathrm{d}x\mathrm{d}y}{z-\zeta} + \sum_k \int_{\Gamma_k} \frac{\sigma_k^{(1)}(\zeta)}{z-\zeta}|\mathrm{d}z|, \quad z \in \tilde{D}. \tag{36}$$

Since Darcy law (24) is valid everywhere in the fluid and in particular also on the both sides of the shock front, a general Rankine-Hugoniot formula [23] (35) determines the front moves with the velocity $V_\perp$ normal to the front and there is a flow of mass along the shock with velocity $V_\parallel$ as it is shown on FIG. 7. They read:

$$V_\parallel = -\mathrm{Re}\frac{\mathrm{disc}\, 2\mathrm{i}\phi}{\mathrm{disc}\, S}, \quad V_\perp = -\mathrm{Im}\frac{\mathrm{disc}\, 2\mathrm{i}\phi}{\mathrm{disc}\, S} \tag{37}$$

The Rankine-Hugoniot condition and the differential form of the Darcy equation (24) are the weak form of the Darcy law. We will comment on specific of their derivation in the case of Darcy's law and the meaning of $V_\parallel$ later.

The following physical principles then uniquely determine positions of shocks and define *a dispersive solution*:

1. *zero vorticitiy and Boutroux-Krichever condition* We demand that the circulation of the fluid around the shock is compensated by the transport of mass by the shock (as is in FIG. 7), such that the net vorticity of the flow is null. In the next section we will show that zero vorticity condition yields $\frac{\mathrm{d}}{\mathrm{d}t}\mathrm{Re}\oint S(z)\mathrm{d}z = 0$ for all closed cycles in the fluid. Condition that the line densities are real

$$\sigma_k^{(1)} = \text{real}, \quad z \in \Gamma, \tag{38}$$

   satisfies this requirement, and furthermore leads to a stronger *Boutroux-Krichever* condition

$$\mathrm{Re}\oint S(z)\mathrm{d}z = 0, \quad \text{all fluid cycles.} \tag{39}$$

2. *admissibility condition* Furthermore, we demand that the line densities are positive, like before the critical time, as discussed in the *inverse balayage* section.

$$\sigma_k^{(1)} > 0. \tag{40}$$

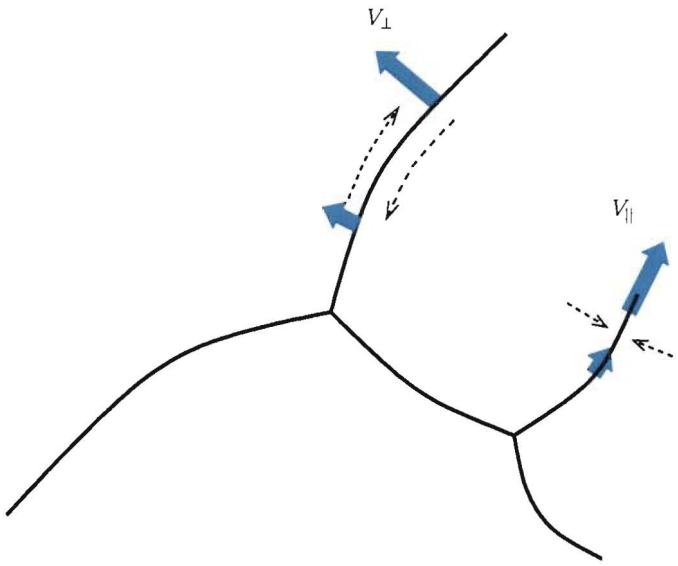

FIG. 7: Vorticity cancellation by normal velocity and mass conservation by parallel velocity. The dashed arrows are the direction of the ambient air (with velocity $\propto \nabla p$) and the thick arrows are the velocity of the compressed air.

This condition means that shocks represent *fluid deficit*. As a result, the shock moves toward the direction of higher pressure as is in FIG. 7.

The *zero vorticity* and admissibility conditions bring Rankine-Hugoniot condition to the form

$$\sigma^{(1)} V_\perp = \operatorname{disc} p, \tag{41}$$

$$\sigma^{(1)} V_\parallel = -\operatorname{disc} \psi \tag{42}$$

Summing up, the condition that the line densities are real and positive uniquely define the weak solution: a graph of shocks given by the condition

$$\Gamma(t): \quad -\text{idisc } S(z,t)\mathrm{d}z = 2\sigma^{(1)}(z,t)|\mathrm{d}z| = \text{real positive}. \tag{43}$$

Dynamics of shocks is determined motion of branch points, which in its own turn is determined by the Darcy Law.The same conditions also determine the motion of the skeleton before and after critical time. After a critical time shocks can be considered as continuation of growth of a skeleton inside the fluid. From this point of view skeleton and shocks together form a graph which grows under the same law. As we will see below, the boundary is singled out as a position of the first branching event. Following branching events already occur in the fluid as branching shocks.

We will demonstrate how it works on a rather general but explicit example, below.

Hydrodynamics of the shocks

Let us further discuss the hydrodynamics of shocks. We integrate equation (24) over a closed loop ∂B drawn anywhere on the plane. If the loop does not cross the skeleton, and adopting the above interpretation when the fluid extends up to a skeleton, we obtain

$$\frac{1}{2}\frac{\mathrm{d}}{\mathrm{d}t}\mathrm{Im}\oint_{\partial B} S(z)dz = -\iint_B \nabla\cdot\rho\mathbf{v}\,\mathrm{d}x\mathrm{d}y = \oint_{\partial B}\rho\mathbf{v}\times\mathbf{dl} = \oint \mathrm{d}\psi, \tag{44}$$

$$\frac{1}{2}\frac{\mathrm{d}}{\mathrm{d}t}\mathrm{Re}\oint_{\partial B} S(z)dz = \iint_B \nabla\times\rho\mathbf{v}\mathrm{d}x\mathrm{d}y = \oint_{\partial B}\rho\mathbf{v}\cdot\mathbf{dl} = \oint \mathrm{d}p, \tag{45}$$

where $\nabla\times\mathbf{v} = \partial_y v_x - \partial_x v_y$ is the vorticity field, and $\nabla\cdot\mathbf{v} = \partial_x v_x + \partial_y v_y$ is the divergence of velocity field ($2\bar{\partial}v = \nabla\cdot\mathbf{v} + i\nabla\times\mathbf{v}$). The first two equalities in each line of (44, 45) are identities, the last is one is the Darcy equation.

Let us now consider the integral $\oint_{\partial B} S(z)dz$ over a loop which does intersect a shock graph (or an extended graph including a skeleton) at one or two points. This integral measures the density of a part of a shock surrounded by the loop and under (43) stays purely imaginary at all times. We conclude that

$$\frac{\mathrm{d}}{\mathrm{d}t}\mathrm{Re}\oint S(z)\mathrm{d}z = 0. \tag{46}$$

Letting the contour now shrink to an infinitesimal loop, we obtain the differential form of (46) in the form

$$\frac{\mathrm{d}}{\mathrm{d}t}\,\mathrm{Re}\,[\mathrm{disc}\,S\;\mathrm{d}z]_{\xi\in\Sigma_k} = 0. \tag{47}$$

The total time derivative in (47) has two contributions, one from the time evolution of the Schwarz function, the other from the motion of the skeleton. We denote the (complex) velocity of the skeleton (normal to the instantaneous curves Σ), by $V_\perp$. Then the total time derivative (47) becomes

$$\mathrm{Re}\,[\mathrm{disc}\,\dot{S}\;\mathrm{d}z + \nabla_{\|}(\mathrm{disc}\,S\cdot V_\perp)|\mathrm{d}z|]_{\xi\in\Sigma_k} = 0, \tag{48}$$

where $\nabla_{\|}$ represents the derivative along the direction tangent to the skeleton.

From the jump condition (43) and the fact that $V_\perp$ is normal to the skeleton, it follows that the second term in (48) is purely real, and equals $2\nabla_{\|}\left(\sigma^{(1)}V_\perp\right)|\mathrm{d}z|$. Here, $V_\perp$ is the algebraic value of the velocity of the shock - positive if directed along the positive normal to the cut as is on FIG.6. For the first term, we use the identity following from Darcy's law (24) on both sides of the cut, $\mathrm{disc}\,\dot{S} = 2\mathrm{i}\;\mathrm{disc}\,\partial_z\phi$, along with the Cauchy-Riemann conditions on both sides, to obtain $\mathrm{Re}\,[\mathrm{disc}\,\dot{S}\;\mathrm{d}z] = 2\mathrm{disc}\;v_{\|}|\mathrm{d}z|$, where $v_{\|}$ is the fluid velocity along the cut.

Together, it yields to the equation

$$\nabla\times\mathbf{J} + \rho\,\mathrm{disc}\;v_{\|} = 0, \quad \mathbf{J} = \sigma^{(1)}\mathbf{V}_\perp \tag{49}$$

The first term in this equation represents the transport of mass due to motion of the shock (normal to the shock itself), while the second is the vorticity of the surrounding oil flow. They compensate each other. Introducing the notation $\rho^{(2)}(\mathbf{r}) = \delta^{(2)}(\mathbf{r}-\xi)\sigma^{(1)}(\xi)$ for the density of sources we may write Eq. (45) for a contour surrounding part of the cuts

$$\iint_B \nabla\times\left(\rho\mathbf{v} + \rho^{(2)}\mathbf{V}_\perp\right)\mathrm{d}x\mathrm{d}y = 0. \tag{50}$$

This equation, derived solely from the condition that $\sigma^{(1)}$ is real, suggests to interpret a shock as a single layer of positive vortices. Then $\sigma^{(1)}$ is the (smooth part of) density of vortices. The core of the vortex is of the order of $\hbar^{1/2}$ - the width of the shock.

Using Darcy law we replace the fluid velocity in (49) by $-\partial_{\|}p$, and integrate (49) along the cut. We get

$$\sigma^{(1)}V_\perp = \mathrm{disc}\;\mathrm{p}. \tag{51}$$

(the constant of integration is fixed from the fact that the density and the discontinuity of pressure vanish at the end of the cut). Here, again $V_\perp = \pm|V_\perp|$ is the algebraic value of the velocity. Notice that the shock moves toward the direction of smaller pressure due to the admissibility condition (57). The latter means that the shock is a position of a deficit of fluid.

Apart from motion of the shock, there is also a stream of mass along the shock. Consider a change of the density between two points ξ and $\xi + \mathbf{V}_\perp\mathrm{d}t + \mathbf{V}_{\|}\mathrm{d}t$. This is Lagrangian time derivative of the line density $\frac{\mathrm{d}}{\mathrm{d}t}\sigma^{(1)}\mathrm{d}t$. It follows from the Eq. (44) that $\dot{\sigma}^{(1)} = \mathrm{disc}\,\nabla_{\|}\psi$ and due to the continuity condition $\dot{\sigma}^{(1)} + \nabla_{\|}(\sigma^{(1)}V_{\|}) = 0$ we determine the sliding velocity $V_{\|}$ and a stream of mass along a shock

$$\sigma^{(1)}V_{\|} = -\mathrm{disc}\,\psi \tag{52}$$

At a branch point $e(t)$ (an and of a shock) the total velocity of the shock matches the velocity of the branch point

$$\dot{e}(t) = \left(V_\perp + V_{\|}\right)|_{z=e(t)}. \tag{53}$$

We notice that at leas close to the end of the the stream of mass is directed toward the branch point.

Later we illustrate the hydrodynamic formulas by direct calculations.

Real complex curve and its differentials

The planar curve – boundary of the fluid, given by the equation (20) – is a real oval (or real section) of the real *complex curve* (finite-genus Riemann surface). If the domain is algebraic, there must be a polynomial $f(z,\tilde{z}) = \sum_{nm} a_{mn} z^n \tilde{z}^m$, $a_{nm} = \overline{a_{nm}}$ such that $\tilde{z} = \rho^{-1} S(z)$ is one out of many solutions of the equation $f(z,\bar{z}) = 0$. The function $f(z,\bar{z}) = 0$ defines a real complex curve. The Schwarz function then represents a particular sheet of this curve which we call physical. The boundary of the domain is then a set when $\tilde{z}$ is equal to $\bar{z}$, called a *real oval.* For a symmetric hypertrocoid, we have $f(z,\bar{z}) = (z\tilde{z})^2 - 4r_c(z^3 + \tilde{z}^3) + 4(r_c^2 - \frac{r^2}{4})(1 + \frac{r^2}{2r_c^2})(z\tilde{z}) - 4r^2(r_c^2 - \frac{r^2}{3})$ [14].

Having real complex curve in mind (not only its real oval) has proved to be useful for studying a Hele-Shaw flow and is necessary to understand its weak solutions. The Hele-Shaw flow of a generalized quadrature domain then understood as the evolution of a meromorphic differential $\mathrm{d}\Omega = S(z)\mathrm{d}z$. The properties described above can be cast as algebro-geometrical properties of the curve:

1. the complex curve is real;

2. condition that all densities are real yields

$$\mathrm{Re} \oint \mathrm{d}\Omega = 0, \quad \text{for all cycles in the fluid;}. \tag{54}$$

3. condition that all densities are positive yields

$$\mathrm{Im}\,\mathrm{disc}\, S\, \widehat{d\ell} > 0, \tag{55}$$

   or equivalently $\mathrm{disc}\,\mathrm{Re}\,\Omega$ is *increasing* away from the cut;

4. shocks form a graph determined by the condition

$$\mathrm{Re}\,\mathrm{disc}\,\Omega = 0, \tag{56}$$

   and the admissibility condition 3. The graph (56) consists of curved lines some times called *anti-Stokes* lines;

5. the meromorphic differential $\mathrm{d}\Omega$ has only multiple poles at infinity, the residues at infinity of the differential $z^{-k}\mathrm{d}\Omega$ are the deformation parameters (9), time is the residue of the differential $\mathrm{d}\Omega$ at infinity.

According to property 3 above, the real part of the *generating function* $\Omega(z) = \int_{z_\gamma}^{z} S(\zeta)\mathrm{d}\zeta$, where z_γ is a chosen point on the boundary, is a single-valued function. The integral of the differential over a cycle involving a drain is $\oint \mathrm{d}\Omega = \mathrm{i}\pi t$.

Being cast in this form the properties of the curve fully and uniquely determine a smooth Hele-Shaw solution before singularity is reached and a weak dispersive solution after the singularity.

As we have discussed the boundary of the fluid before it reaches a singularity is a degenerate curve. A singularity occurs when a branch point meets a double point on a boundary, forming a triple (or higher order) point, so the curve further degenerates, while the boundary of the real oval forms a cusp. Beyond this time the triple degenerate point splits into three regular branch points, such as the curve becomes non-degenerate. In other words going through a singularity the curve changes the genus. This process is illustrated by the FIG.8.

An evolution of curve obeying Krichever-Boutroux condition through a change of a genus has been appeared in studies of Whitham averaging in integrable systems by Krichever [40]. Recently a similar condition has been recognized in the theory of orthogonal polynomials by Bertola and Mo [41, 42]. Both appearances are not a coincident. Semiclassical asymptotes of orthogonal polynomials and Whitham genus changing transition are ultimately related to the Hele-Shaw flow [14, 16, 43?].

As we have said close to a cusp-singularity a complex curve locally is a hyperelliptic (18). It describes a finger moving toward a cusp. In this case the residue of the pole at infinity t_1 in Eq. (18) is $t_c - t$ - the time before the cusp singularity. Also in the hyperelliptic case $\mathrm{Im}\,\Omega$ on both sides of the cuts has opposite signs, while $\mathrm{Re}\,\Omega$ is zero on the cut. For hyperelliptic curve we can replace the property 55 by the condition

$$\mathrm{Re}\,\Omega(z) > 0, \tag{57}$$

in the neighborhood of the cut.

In the case of a hyperelliptic curve $Y^2 = R_{2l+1}(X)$, the meromorphic differential entering the weak solution reads

$$\mathrm{d}\Omega = \mathrm{i}Y\mathrm{d}X. \tag{58}$$

In this case any closed cycle $\mathcal{C}$ in the fluid domain may represent either a closed path on one of the two sheets $Y > 0$, or $Y < 0$ (if it does not cross any branch cut), or an open path on the complex curve, if it crosses branch cuts Γ. Crossing the branch cut at a point (X, Y) brings the path to the second sheet of the complex curve. In order to close the path it is necessary to cross the cut once more, so that the total path becomes $(X, Y) \to (X, -Y) \to (X, Y)$. We use this convention in the next section.

BEYOND (2,3)-CUSP SINGULARITY: SELF-SIMILAR WEAK SOLUTION

In this section, we give a detailed analysis of the generic cusp singularity and illustrate a nature of weak solution. The computations below describe the evolution of a unique elliptic Krichever-Boutroux curve. We comment that part of this analysis appeared in paper [44] which is devoted to Whitham averaging of the *physical* solution [?] of Painleve I equation. In this section we set $\rho = 1$.

Ellipic curve; genus transition

As we have said, in the vicinity of the (2,3) cusp a complex curve is a real elliptic curve. Before a critical time (which we set $t = 0$) the real oval of the curve (a set of real X and Y) describes a finger evolving toward the cusp.

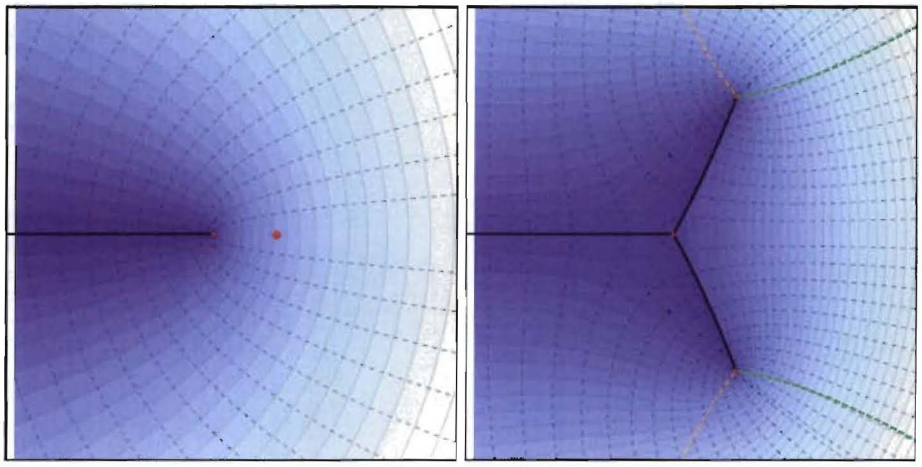

FIG. 8: The equi-pressure lines and the flow (dashed) lines before the critical time (left), and after the critical time (right). Also drawn are the equi-pressure lines (contour lines) and the flow lines (dashed lines). Pressure of oil gets larger as the shade gets darker. The boundary of the fluid is a very narrow finger $y^2 \sim x^3$ around the skeleton line (the thick line on the real axis) and it is not depicted. The red dots are the branch points, $e_{1,2,3}$. Real e_3 is the tip of the finger. Before the critical time $e_2 = e_1$ is the double point (larger red dot in left figure). The thick lines (on the right figure) connecting the branch points are the shocks. In the right figure, the orange and green dashed lines that emanates from the branch points are the level lines of $\mathrm{Re}\,\Omega$. The fluid is flowing to the lighter region toward low pressure.

FIG. 8 illustrate the genus transition of the curve and hydrodynamics of shocks. We depict the X-plane where the boundary of the fluid domain coincide with a skeleton $\mathrm{Im}X = 0$, $\mathrm{Re}X < e_3$.

Before the critical time two branch points are coincide in the fluid. There pressure and velocity are smooth. The branch point e_3 is a tip of the finger. At the critical time the tip meets the double point. After the critical point the double point splits into two branch points which occur in the fluid. They are the end of the shocks. The tip of the finger e_3 retreats. Fluid goes toward lower pressure (lighter regions) creating a deficit on shocks where fluid decompresses. Shocks move in the opposite direction toward higher pressure (darker regions).

We write the curve as

$$Y^2 = -(4X^3 - g_2(t)X - g_3(t)) = -4(X - e_3(t))(X - e_2(t))(X - e_1(t)). \tag{59}$$

where $e_3(t)$, $e_2(t)$, $e_1(t)$ are time dependent branch points. One root, say e_3 can be always chosen to be real. Other two then are complex conjugated $e_2 = \bar{e}_1$. The coefficient in front of X^2 is removed by translation such that $e_3+e_2+e_1 = 0$. An evolution of roots is determined by the Darcy law (26). We set the time $t = 0$ at the moment of cusp formation.

The positive part of the curve is $\pm Y_+ = i2X^{3/2} - i\frac{g_2}{4}X^{-1/2}$. The coefficient of $X^{-1/2}$-term is determined by the behavior of the pressure at the infinity. Under this setting

$$-\frac{1}{4}g_2 = -e_3^2 + |e_2|^2 = 3t, \quad g_3 = 4e_3|e_2|^2, \quad e_3 = -2\mathrm{Re}\, e_2. \tag{60}$$

It follows that the roots scale as $t^{1/2}$, while X and Y scales as $t^{1/2}$ and $t^{3/2}$.

A comment is in order: the elliptic curve (59) only approximately describe the finger as $t \to 0$; since X and Y have different scaling, a complex coordinate of a physical plane $z = X + iY$ must be treated just as $z = X$. A map $u \to X$ covers the physical plane twice as it is shown on FIG.9. For the same reason

1. Before the critical time ($t < 0$) the real branch point e_3 is negative. It is located outside of the fluid. Therefore $\mathrm{Re}\, e_2 > 0$. and then lay in the fluid. Condition that the curve must have no branch points in the fluid (followed from incompressibility of the fluid) requires that two branch points coincide: $e_2 = e_1 = -e_3/2 > 0$, so that the curve is degenerate as is in (14). Condition (60) yields

$$e_3 = -2\sqrt{-t}\,, \qquad e_2 = e_1 = \sqrt{-t}. \tag{61}$$

   The double point $e_2 = e_1$ located in the fluid and the branch point e_3 located outside of the fluid are depicted in Fig.8. The curve reads: $Y^2 = -(4X^3+12tX+8(-t)^{3/2})$ [15]. The skeleton is a real half axis $\mathrm{Im}X = 0$, $\mathrm{Re}X < e_3$.

2. At the critical time $t = 0$ all roots coincide $e_3 = e_2 = e_1 = 0$. The curve further degenerate to a cusp $Y^2 = -4X^3$. the skeleton touches the the double point.

3. After the critical time $t > 0$, we push the evolution by splitting the double point $e_2 \neq e_1$. The new branch points appeared in the fluid giving rise to shocks. By the previous argument, we only need to determined the constant term $g_3 = 4e_3|e_2|^2$. Unique solution exists such that the integral of the differential

$$\oint \mathrm{d}\Omega \equiv -\mathrm{i}\oint Y\, dX = \text{imaginary} \tag{62}$$

   over all the cycles are purely imaginary.

   To get the solution let us parametrize the curve $Y(X)$ by a uniformizing coordinate u as

$$X = \wp(u) \tag{63}$$
$$Y = \mathrm{i}\wp'(u). \tag{64}$$

   where $\wp$ is the Weierstrass elliptic function which half-periods $\omega(t)$ and $\omega'(t)$ are yet to be determined complex functions of time. Since e_3 is real $\omega + \omega'$ is real, and $e_2 = \bar{e}_1$ then $\omega = \bar{\omega}'$. They scaled with time as $\omega \sim t^{-1/4}$. The branch points are given by $(e_3, e_2, e_1) = (\wp(\omega+\omega'), \wp(\omega), \wp(\omega'))$. The rhombus-shape fundamental domain depicted in FIG. 9 [48].

   The potential of the flow is obtained from the Darcy's law by

$$\phi(X) = -\int_{e_3}^{X} dX\, \partial_t Y = 6\mathrm{i}\left(\zeta(u) - \frac{3}{2}\frac{g_3}{g_2}u\right)\,, \qquad g_2 = -12t\,. \tag{65}$$

   The stream function, $\psi = \mathrm{Re}\,\phi$, and the pressure, $p = \mathrm{Im}\,\phi$, will be read from $\phi(X)$. Here we have used the facts:

$$u = \mathrm{i}\int^{X} \frac{dX}{Y(X)}\,, \qquad \zeta(u) = -\mathrm{i}\int^{X} \frac{X dX}{Y(X)}\,, \tag{66}$$

   up to constants of integration. The generating function $\Omega = -\mathrm{i}\int_{e_3}^{u} Y\mathrm{d}X$ reads

$$\Omega(u) = -\mathrm{i}\int_{e_3}^{X} Y\, dX = \int_{\omega-\omega'}^{u} \wp' d\wp = \frac{2}{5}\wp'\wp - \frac{24t}{5}\left(\zeta - \frac{3}{2}\frac{g_3}{g_2}u\right)\,. \tag{67}$$

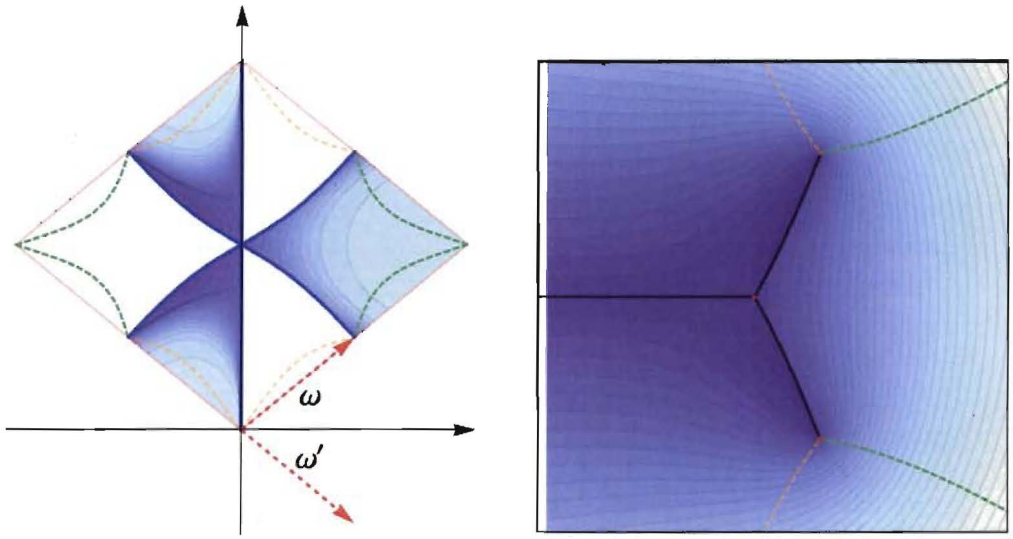

FIG. 9: Fundamental domain u (left) and physical X-plane (right). The pressure level-lines are drawn in both planes. The region without contour shading in u-plane, maps to the unphysical plane. The dashed (orange and green) lines are level lines of $\mathrm{Re}\,\Omega$ emanating from the branch points. The thick lines are the admissible anti-Stokes lines - shocks.

The Krichever-Boutroux condition (62) determines the curve, i.e. g_3. On u-plane the **b**-cycle condition can be written as $\mathrm{Re}\,[\Omega(\omega+\omega')-\Omega(0)]=0$ and it amounts to

$$\phi(\omega+\omega')=0 \quad \Leftrightarrow \quad \frac{3}{2}\frac{g_3}{g_2}=\frac{\zeta(\omega+\omega')}{\omega+\omega'} \tag{68}$$

or, equivalently, $\frac{3}{2}\frac{g_3}{g_2}=\frac{\mathrm{Re}\,\zeta(\omega)}{\mathrm{Re}\,\omega}$, where we used the identity $\zeta(\omega+\omega')=\zeta(\omega)+\zeta(\omega')$.
The scaling properties of the curve and the hydrodynamics are summarized as

$$X(u,t)=t^{1/2}x_1(t^{1/4}u)\,, \tag{69}$$
$$Y(u,t)=t^{3/4}y_1(t^{1/4}u)\,, \tag{70}$$
$$\phi(u,t)=t^{1/4}\phi_1(t^{1/4}u)\,, \tag{71}$$
$$v(u,t)=t^{-1/4}v_1(t^{1/4}u)), \tag{72}$$
$$N(t)=t^{1/2}N_1 \tag{73}$$

where the functions subscripted by 1 are those evaluated at $t=1$.
The velocity $v=v_x-\mathrm{i}v_y$ is written by the above using $v_1(u)$ that is defined by

$$v_1(u)=\mathrm{i}\frac{\partial_u\phi(u)}{\partial_u X(u)}=6\frac{\wp(u)+\frac{3}{2}\frac{g_3}{g_2}}{\wp'(u)}\,. \tag{74}$$

Solution of this equatin may be found in Ref. [44]. The unique elliptic curve is summarized as follows:

$$\begin{aligned}(e_3,e_2,e_1)&=\sqrt{\frac{12}{4h^2-3}}(\tfrac{1}{2}+\mathrm{i}h,\tfrac{1}{2}-\mathrm{i}h,-1)\sqrt{t}\\ g_2&=-12\,t\\ g_3&=-12\sqrt{\frac{12}{4h^2-3}}\frac{4h^2+1}{4h^2-3}\,t^{3/2}\approx -7.321762431\,t^{3/2},\end{aligned} \tag{75}$$

where $h\approx 3.246382253744278875676$. This number comes from $m=\frac{1}{2}+\frac{3}{2}\frac{1}{\sqrt{9+4h^2}}$ where m is the solution of the equation

$$(16m^2-16m+1)E(m)=(8m^2-9m+1)K(m)\,, \tag{76}$$

· that follows from (68). Here E and K are elliptic integrals. They also determine a shape of the fundamental domain

$$\frac{\mathrm{Im}\,\omega}{\mathrm{Re}\,\omega} = \frac{K'(m)}{K(m)} \approx 0.81736372$$

In brief the genus transition is summarized by an abrupt change of g_3

$$g_3 = |t|^{3/2} \begin{cases} -8, & t < 0, \\ -7.321762431, & t > 0. \end{cases} \tag{77}$$

This discontinuity is related to the **capacity** C (an analog of conformal radius) of elliptic curve which is defined by an asymptote of the potential ϕ at $X \to \infty$:

$$\phi(X) = -6\mathrm{i}X^{1/2} - \mathrm{i}\frac{C}{2X^{1/2}} + \ldots \tag{78}$$

where C is given by

$$C = \dot{g}_3 = \frac{3}{2}|t|^{1/2} \begin{cases} 8, & t < 0, \\ -7.321762431, & t > 0. \end{cases} \tag{79}$$

One can see that, at $t = 0$, the capacity C goes through a discontinuous jump on its coefficient.

We mention few major steps to derive the equation (76) from (68). We use the following formula from [45] **Abramowitz and Stegun: Handbook of Mathematical Functions page 649**:

$$\zeta(\omega + \omega') = \frac{K(m)}{3(\omega + \omega')}\left[6E(m) + (4m - 5)K(m)\right] , \tag{80}$$

$$g_2 = \frac{4(16m^2 - 16m + 1)K^4(m)}{3(\omega + \omega')^4} , \tag{81}$$

$$g_3 = \frac{8(2m - 1)(32m^2 - 32m - 1)K^6(m)}{27(\omega + \omega')^6} . \tag{82}$$

Simply plugging in the above formula to (68) one gets (76) immediately. We also mention that all the formula for the branch points can also be found in the same reference.

Shock lines are given by the condition (56) or, in our case, simply by

$$\mathrm{Re}\,\Omega(X) = 0 . \tag{83}$$

Given $Y(X)$, there are only a finite number of candidates for shock configuration. Without breaking the up-down symmetry, there are only **three** ways to configure the branch cuts. Among those three possibilities, only the case described above has *finite shock* and *no abrupt change at infinity*. We discard the other two cases either by the physical intuition that the shock must have a finite mass, or by imposing the boundary condition at the infinity. For a curious reader, the other two cases are when the cuts are chosen to be i) all the level lines and ii) the one in the real line and the two that go to the directions $\sim \pm 3\pi/5$ near infinity. Note that we have seven level lines to consider: five lines that go to infinity and two finite ones.

Detailed description of the shock

It is interesting to follow zero-pressure line. It always emanates from the branch points. Before the critical time it is also a boundary of the fluid. After the critical time a zero pressure line has two branches. One remains close to the boundary of the two fluids, another branch is in the fluid and crosses the boundary at a point where $\mathrm{d}\phi = 0$ as is on FIG. 8. This occurs at $x = -\frac{\zeta(\omega+\omega')}{\omega+\omega'} = -\frac{3}{2}\frac{g_3}{g_2}$. The zero-pressure line emanates from the branch point e_1 with the angle $\theta_{\text{equi-pressure}} \approx 1.235\pi$, as we will evaluate soon.

The significance of the point $d\phi = 0$ and the zero-pressure line can be seen at FIG. 10. One can see that the stream lines (dotted lines) of oil that start from the real cut, flow in the opposite directions with respect to the zero-pressure line: the one in the right goes to real cut, the one in the left goes out of the real cut. Exactly at $d\phi = 0$ the flow lines are intersecting perpendicularly. It is also a stationary point of oil where the velocity of oil flow becomes zero.

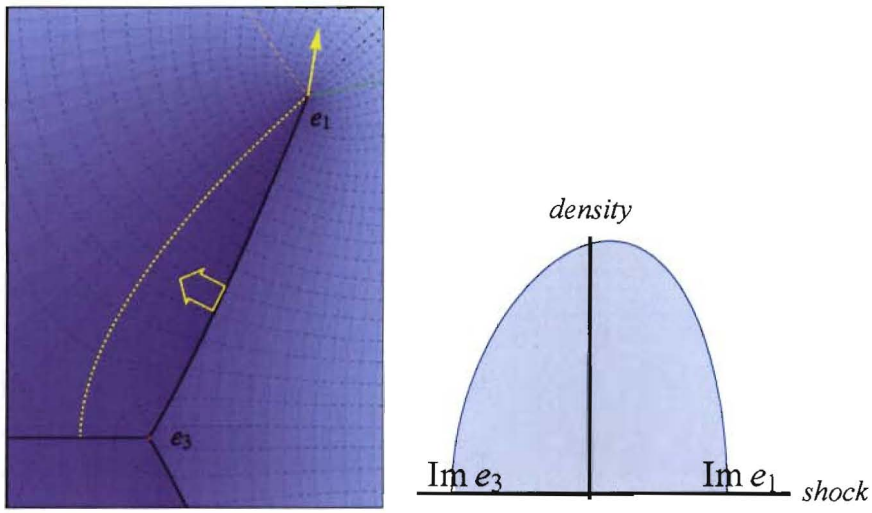

FIG. 10: The close-up of shocks (left) and the line density profile of the shock (right). In the left, the shaded contours are equi-pressure lines and the dashed lines are the stream lines. The darker the shade is, the higher is the pressure in the fluid. The yellow dotted line is the zero-pressure line; it crosses the boundary of the fluid and a skeleton. With respect to this line, the main cut release/absorbs oil: on the left of the zero-pressure line the real cut releases oil, on the right the real cut absorbs oil. The line density on the shock vanishes at the branch points as square root. Also by the self-similarity, the total charge on the shock grows exactly by $\int_{e_1}^{e_3} y\,dx \propto t^{5/2}$. The red arrow is the moving direction of the branch point. At e_3 three directions: equi-pressure line, shock, the velocity, are all at different angles; see the text.

As has been pointed out, the evolution of the curve $Y(X)$ is self-similar: the whole picture in FIG. (8) simply expands with respect to the origin by the factor $\sqrt{t}$ for $t > 0$ (or $\sqrt{-t}$ for $t < 0$). Therefore, the branching shocks are moving to the darker region (to the left) as time goes on (see the big arrow for the motion of the shock).

In FIG. 8 the cuts are located by the condition $\mathrm{Re}\,\Omega = 0$. We have argued that this condition leads to the curl-free flow of the *entire fluid* which after the critical time consists of **anti-compressed** fluid in the shock and a fluid with a constant density elsewhere.

Let us discuss a behavior of physical quantities around branch points, say e_1. The line density is given by

$$\sigma^{(1)} = |Y| \sim 2\left|\sqrt{-(e_1-e_2)(e_1-e_3)}\sqrt{X-e_1}\right| \approx 2|\gamma|\sqrt{t}\sqrt{|X-e_1|}\,, \tag{84}$$

where $|\gamma| \approx 2.66757$ comes from the estimate below.

$$\gamma = \frac{1}{t}\sqrt{-(e_1-e_2)(e_1-e_3)} = \sqrt{\frac{12(2h^2-3\mathrm{i}h)}{4h^2-3}} \approx 2.60534 - \mathrm{i}0.57281\,. \tag{85}$$

From this we can estimate the angle of the shock (and all the anti-Stokes lines) θ_{shock} at e_1 by

$$\frac{3}{2}\theta_{\mathrm{shock}} + \arg\gamma \equiv 0 \mod 2\pi \quad \Rightarrow \theta_{\mathrm{shock}} \approx 0.45326\pi - \frac{2}{3}\pi\,. \tag{86}$$

The angles of the other two anti-Stokes lines are obtained by adding (subtracting) $\frac{2}{3}\pi$ to the above.

We also estimate the density near e_3.

$$\sigma^{(1)} = |Y| \sim 2\left|\sqrt{-(e_3-e_1)(e_3-e_2)}\sqrt{X-e_3}\right| \approx 2\sqrt{|t|}\sqrt{|X-e_3|} \times \begin{cases} 3 & t<0 \\ 1.97975 & t>0 \end{cases} \tag{87}$$

This indicates the discontinuous change similar to the behavior of the capacity (79).

The graph of the density is depicted in FIG. 10. The total mass deficit carried by the shock is

$$\left|\int_{e_1}^{e_3} Y\,dX\right| = \frac{4}{5}\left|\mathrm{Re}\,\phi_{X=e_3}^{X=e_1}\right| t \approx \frac{4}{5}(6.34513)\,t^{5/4}\,.$$

Simple calculations give the potential (pressure and the stream function) at the branch point.

$$\phi(X) \sim e_1\sqrt{-(e_1-e_2)(e_1-e_3)}\sqrt{X-e_1} \approx (1.7506 + \mathrm{i}4.5237)\, t\sqrt{X-e_1}\ . \tag{88}$$

The above can yield the angle of the zero-pressure line to be

$$\frac{1}{2}\theta_{\text{zero-pressure}} + \arg(1.7506 + \mathrm{i}4.5237) = 0 \quad \Rightarrow \quad \theta_{\text{zero-pressure}} = -0.764939\pi\ . \tag{89}$$

The velocity of the branch points are determined by the scaling relation (69) $\dot{e}_k = \frac{1}{2}e_k$, $k = 1, 2, 3$. They are depicted by the red arrow in FIG. 10.

The contribution to the power $N(t)$ from the shock is given by the line integral that tightly surrounding the shock:

$$N(t)_{\text{shock}} \sim -K \oint_{\text{shock}} p\nabla p \times d\ell = K \oint_{\text{shock}} (\operatorname{Im}\phi)\operatorname{Re}(\partial_u \phi\, du) \approx 3.1207K\sqrt{t}\ , \tag{90}$$

on a single side of a single shock.

Acknowledgments

This work was carried out under the auspices of the National Nuclear Security Administration of the U.S. Department of Energy at Los Alamos National Laboratory under Contract No. DE-AC52-06NA25396. R.T. acknowledges support from the Center for Nonlinear Studies at LANL, and the LDRD Directed Research grant on *Physics of Algorithms*. Hospitality of the Aspen Center for Physics, the Centre for Mathematical Research, Montreal, Canada, and the Galileo Galilei Institute in Florence, Italy is also gratefully acknowledged.

[1] H. S. S. Hele-Shaw. *Nature*, 58(1489):34–36, 1898.
[2] H. Darcy. *Fontaines publiques de la ville de Dijon.* Librairie des Corps Impériaux des Ponts et Chaussées et des Mines, Paris, 1856.
[3] Y. E. Hohlov and S. D. Howison. On the classification of solutions to the zero-surface-tension model for Hele-Shaw free boundary flows. *Quart. Appl. Math.*, 51(4):777–789, 1993.
[4] B. Gustafsson and A. Vasil'ev. *Conformal and potential analysis in Hele-Shaw cells.* Advances in Mathematical Fluid Mechanics. Birkhäuser Verlag, Basel, 2006.
[5] P. G. Saffman and G. Taylor. The penetration of a fluid into a porous medium or Hele-Shaw cell containing a more viscous liquid. *Proc. Roy. Soc. London. Ser. A*, 245:312–329. (2 plates), 1958.
[6] B. Shraiman and D. Bensimon. Singularities in nonlocal interface dynamics. *Phys. Rev. A*, 30(5):2840–2842, 1984.
[7] S. D. Howison, J. R. Ockendon, and A. A. Lacey. Singularity development in moving-boundary problems. *Quart. J. Mech. Appl. Math.*, 38(3):343–360, 1985.
[8] S. Richardson. Hele Shaw flows with a free boundary produced by the injection of fluid into a narrow channel. *Journal of Fluid Mechanics*, 56:609–618, 1972.
[9] M. Mineev-Weinstein, P. B. Wiegmann, and A. Zabrodin. Integrable structure of interface dynamics. *Physical Review Letters*, 84:5106, 2000.
[10] I. K. Kostov, I. Krichever, M. Mineev-Weinstein, P. Wiegmann, and A. Zabrodin. tau-function for analytic curves. *MSRI PUBLICATIONS*, 40:285, 2001.
[11] A. Marshakov, P. Wiegmann, and A. Zabrodin. Integrable structure of the Dirichlet boundary problem in two dimensions. *Communications in Mathematical Physics*, 227:131, 2002.
[12] O. Agam, E. Bettelheim, P. Wiegmann, and A. Zabrodin. Viscous fingering and a shape of an electronic droplet in the Quantum Hall regime. *Physical Review Letters*, 88:236801, 2002.
[13] I. Krichever, M. Mineev-Weinstein, P. Wiegmann, and A. Zabrodin. Laplacian growth and Whitham equations of soliton theory. *PHYSICA D*, 198:1, 2004.
[14] R. Teodorescu, E. Bettelheim, O. Agam, A. Zabrodin, and P. Wiegmann. Normal random matrix ensemble as a growth problem. *Nuclear Physics B*, 704:407, 2005.
[15] R. Teodorescu, A. Zabrodin, and P. Wiegmann. Unstable fingering patterns of Hele-Shaw flows as a dispersionless limit of the KdV hierarchy. *Physical Review Letters*, 95:044502, 2005.
[16] E. Bettelheim, O. Agam, A. Zabrodin, and P. Wiegmann. Singular limit of Hele-Shaw flow and dispersive regularization of shock waves. *Physical Review Letters*, 95:244504, 2005.
[17] S-Y. Lee, E. Bettelheim, and P. Wiegmann. Bubble break-off in Hele-Shaw flows : Singularities and integrable structures. *PHYSICA D*, 219:22, 2006.

[18] E. Sharon, M. G. Moore, W. D. McCormick, and H. L. Swinney. Coarsening of fractal viscous fingering patterns. *Phys. Rev. Lett.*, 91(20):205504, 2003.
[19] S. G. Lipson. Pattern formation in drying water films. *Physica Scripta*, T67:63–66, 1996.
[20] T. A. Witten and L. M. Sander. Diffusion-limited aggregation, a kinetic critical phenomenon. *Phys. Rev. Lett.*, 47(19):1400–1403, 1981.
[21] M. B. Hastings and L. S. Levitov. Laplacian growth as one-dimensional turbulence. *PHYSICA D 116*, 244, 1998.
[22] L. D. Landau and E. M. Lifshits. *Teoreticheskaya fizika. Tom VI.* "Nauka", Moscow, third edition, 1986. Gidrodinamika. [Fluid dynamics].
[23] H. Lamb. *Hydrodynamics.* Cambridge Mathematical Library. Cambridge University Press, Cambridge, sixth edition, 1993.
[24] X. Cheng, L. Xu, A. Patterson, H. M. Jaeger, and S. R. Nagel. Towards the zero-surface-tension limit in granular fingering instability. *Nature Physics*, 4:234–237, March 2008.
[25] P. Ya. Polubarinova-Kochina. *Dokl. Acad. Nauk SSSR*, 47:254–7, 1945.
[26] M. B. Mineev-Weinstein and S. P. Dawson. Class of nonsingular exact solutions for Laplacian pattern formation. *Phys. Rev. E*, 50(1):R24–R27, 1994.
[27] S. R. Bell. The Bergman kernel and quadrature domains in the plane. In *Quadrature domains and their applications*, volume 156 of *Oper. Theory Adv. Appl.*, pages 61–78. Birkhäuser, Basel, 2005.
[28] L. A. Galin. *Dokl. Acad. Nauk SSSR*, 47(1-2):250–3, 1945.
[29] S. Tanveer. The effect of surface tension on the shape of a Hele-Shaw cell bubble. *Phys. Fluids*, 29(11):3537–3548, 1986.
[30] S. D. Howison. Cusp development in Hele-Shaw flow with a free surface. *SIAM J. Appl. Math.*, 46(1):20–26, 1986.
[31] J. R. King, A. A. Lacey, and J. L. Vázquez. Persistence of corners in free boundaries in Hele-Shaw flow. *European J. Appl. Math.*, 6(5):455–490, 1995. Complex analysis and free boundary problems (St. Petersburg, 1994).
[32] R. Teodorescu and P. Wiegmann. in preparation.
[33] R. Teodorescu, P. Wiegmann, and A. Zabrodin. Critical points of random matrix ensembles, fingering instability and finite-time singularities. *unpublished.*
[34] M. Sakai. Regularity of a boundary having a Schwarz function. *Acta Math.*, 166(3-4):263–297, 1991.
[35] B. Gustafsson. Lectures on balayage. In *Clifford algebras and potential theory*, volume 7 of *Univ. Joensuu Dept. Math. Rep. Ser.*, pages 17–63. Univ. Joensuu, Joensuu, 2004.
[36] P. D. Lax. Nonlinear hyperbolic equations. *Comm. Pure Appl. Math.*, 6:231–258, 1953.
[37] P. D. Lax. Hyperbolic systems of conservation laws ii. *Comm. Pure Appl. Math.*, 10:537–566, 1957.
[38] P. D. Lax. Development of singularities in solutions of nonlinear hyperbolic partial differential equations. *J. of Math. Phys.*, 5:611–613, 1964.
[39] O. A. Oleinik. Discontinous solutions of non-linear differential equations. *Uspekhi Mat. Nauk*, 12(3):3–73, 1957.
[40] I. M. Krichever. The τ-function of the universal Whitham hierarchy, matrix models and topological field theories. *Comm. Pure Appl. Math.*, 47(4):437–475, 1994.
[41] M. Bertola and M. Y. Mo. Commuting difference operators, spinor bundles and the asymptotics of pseudo-orthogonal polynomials with respect to varying complex weights. *[arXiv.org:math-ph/0605043]*, 2006.
[42] M. Bertola and M. Y. Mo. Isomonodromic deformation of resonant rational connections. *[arXiv.org:nlin/0510011]*, 2005.
[43] S.-Y. Lee, R. Teodorescu, and P. Wiegmann. *in preparation.*
[44] F. Fucito, A. Gamba, M. Martellini, and O. Ragnisco. Non-linear WKB analysis of the string equation. *International Journal of Modern Physics B*, 6:2123, 1992.
[45] D. Aharonov and H. S. Shapiro. Domains on which analytic functions satisfy quadrature identities. *J. Analyse Math.*, 30:39–73, 1976.
[46] In experiments of Ref.[19] the liquid evaporates uniformly including the boundary
[47] We refer an earlier attempt to find a weak solution of the incompressible Hele-Shaw problem in fluid [3, 7, 30, 31]. We do not comment on these interesting papers except stressing that solutions we discuss below are different.
[48] Notations are from Abramowitz and Stegun. See also at `http://mathworld.wolfram.com/Half-Period.html`.